Pergamon

Geochimica et Cosmochimica Acta, Vol. 65, No. 15, pp. 2509–2525, 2001

0016-7037/01 $20.00 + .00

PII S0016-7037(01)00613-5

# The geochemistry of late Archaean microbial carbonate: Implications for ocean chemistry and continental erosion history

BALZ S. KAMBER[1,*] and GREGORY E. WEBB[2]

[1]Department of Earth Sciences, University of Queensland, Brisbane Qld 4072, Australia
[2]School of Natural Resource Sciences, Queensland University of Technology, Brisbane Qld 4001, Australia

(*Received July* 20, 2000; *accepted in revised form February* 23, 2001)

**Abstract**—Trace element concentrations and combined Sr- and Nd-isotope compositions were determined on stromatolitic carbonates (microbialites) from the 2.52 Ga Campbellrand carbonate platform (South Africa). Shale-normalised rare earth element and yttrium patterns of the ancient samples are similar to those of modern seawater in having positive La and Y anomalies and in being depleted in light rare earth elements. In contrast to modern seawater (and microbialite proxies), the 2.52 Ga samples lack a negative Ce anomaly but possess a positive Eu anomaly. These latter trace element characteristics are interpreted to reflect anoxic deep ocean waters where, unlike today, hydrothermal Fe input was not oxidised, and scavenged and rare earth elements were not coprecipitated with Fe-oxyhydroxides. The persistence of a positive Eu anomaly in relatively shallow Campbellrand platform waters indicates a dramatic reversal from hydrothermally dominated (Archaean) to continental erosion-dominated (Phanerozoic) rare earth element flux ratio. The dominant hydrothermal input is also expressed in the initial Sr- and Nd-isotope ratios. There is collinear variation in Sr-Nd systematics, which range from primitive values ($^{87}Sr/^{86}Sr$ of 0.702386 and $\varepsilon_{Nd}$ of +2.1) to more evolved crustal ratios. Mixing calculations show that the range in trace element ratios (e.g., Y/Ho) and initial isotope ratios is not a result of contamination by trapped sediment, but that the chemical and isotopic variation reflects carbonate deposition in an environment where different water masses mixed. Calculated Nd flux ratios yield a hydrothermal input into the 2.52 Ga oceans one order of magnitude larger than continental input. Such a change in flux ratio most likely required substantially reduced continental inputs, which could, in turn, reflect a plate tectonic causation (e.g., reduced topography or expansion of epicontinental seas). 

## 1. INTRODUCTION

Inventories of trace elements and radiogenic isotope signatures in seawater represent the balance between different input sources, and for elements with intermediate residence times, also represent advection of water masses. In modern seawater, continental trace element input via rivers and dust dominates over oceanic hydrothermal input and other sources, such as expelled diagenetic fluids. Veizer et al. (1982), based on the observation of very unradiogenic Sr in some Archaean marine precipitates, popularised the view that balance between continental and hydrothermal inputs could have been dramatically reversed in the first half of Earth's history, with Archaean waters dominated by hydrothermal inputs. Derry and Jacobsen (1988) proposed that the Proterozoic eon saw a significant transition from mantle-dominated (i.e., hydrothermal) ocean chemistry to a modern system. Although the observation of such a transition is undisputed, the underlying geologic factors that caused the change are largely unknown. Of particular interest is the question of whether the change in balance was caused solely by temporal decline of the hydrothermal flux (related to decline of oceanic crust production rate) or whether mass balance also requires severely inhibited continental flux to Archaean oceans with obvious implications for continental erosion.

Reliable trace element data combined with Sr- and Nd-isotope proxies for Archaean seawater have the potential to provide new insights. However, because marine chemical precipitates can be subject to contamination by detritus and volcanic ash and have experienced diagenesis, it is not surprising that views regarding geochemistry and isotope composition of the Archaean oceans differ widely between continent-dominated (e.g., Miller and O'Nions, 1985) and hydrothermal-dominated systems (e.g., Derry and Jacobsen, 1990). Here we present combined trace element Sr- and selected Nd-isotope data for late Archaean microbialites, following an earlier study (Webb and Kamber, 2000) wherein we successfully tested the feasibility of the microbialite proxy using Holocene examples from the Great Barrier Reef. We argue that the trace element chemistry of the stromatolites faithfully records that of ancient ambient seawater. Continental or volcanic contamination can be monitored, and diagenetic effects evidently did not overprint the chemical signature of the well-preserved carbonate precipitates. Our data provide evidence for much reduced continental input into the oceans during the late Archaean. We test whether reduction in continental flux was proportional to the smaller late Archaean continental mass and speculate about the consequences for tectonic models.

## 2. MICROBIALITES, STRATIGRAPHY, SAMPLING STRATEGY, AND METHODS

### 2.1. Microbialites and Stratigraphy

The term microbialite refers to a class of sedimentary structures wherein minerals were precipitated or localised as a byproduct of

*Author to whom correspondence should be addressed (kamber@earthsciences.uq.edu.au).

metabolic activities or decay processes of microbial communities and/or associated organic matter. Although trapping and binding of sediment grains may occur in microbialites, many such structures consist almost entirely of minerals precipitated directly from ambient waters (Riding, 1991). The geochemistry of microbialites is complicated by trapped sediments. Trapped siliciclastic sediments have high trace element contents (compared to carbonate) that may completely mask seawater-derived patterns, but such contamination is readily detectable (Webb and Kamber, 2000). Trapped skeletal carbonate sediment is less problematic owing to its typically very low trace element content. However, skeletal carbonates may not incorporate trace metals from seawater proportionally and, therefore, may be more difficult to detect. Precambrian microbialites have the advantage that any trapped carbonate sediments are likely to represent abiotic precipitates or other microbial sediments, both of which are expected to incorporate trace elements in proportion to seawater, regardless of concentration. Stromatolites, which are characterised by laminated internal structure, are the best-known microbialites. Well-preserved stromatolites occur throughout the geologic record and dominated the fossil record throughout most of the Precambrian.

The present study used six stromatolite-bearing samples from the Campbellrand Subgroup, Transvaal Supergroup, South Africa. An interlayered volcanic tuff bed in the Campbellrand subgroup was dated to $2521 \pm 3$ Ma (Sumner and Bowring, 1996; see Fig. 1) and thus was deposited at the boundary between the Archaean and Proterozoic eons. The sedimentology of the spectacular Campbellrand Subgroup has been the subject of numerous studies (e.g., Beukes, 1987; Hälbich et al., 1992; Sumner, 1997a). Those investigators agreed that the stromatolite-rich carbonates of the Campbellrand Subgroup and the correlative Malmani subgroup were deposited on a large, shallow marine platform that is interpreted to have covered most of the present-day Kaapvaal continent. Cements from the vast carbonate platform formed in a relatively clean environment in terms of continental detritus and volcanic ash. However, intermittent deposition of shale higher in the stratigraphy (Hälbich et al., 1992; Fig. 1) implies that relatively proximal continental sediment sources did exist.

Carbonates at the edge of the platform are interpreted to have been deposited in water depths exceeding several tens of meters, but most of the platform represents shallow, subtidal to peritidal environments (Beukes, 1987; Sumner, 1997a). The suite of samples used in the present study represents the full range in water depth. Samples 5 and 6 are microbially laminated stromatolites from the uppermost Kogelbeen Formation, which according to Sumner (1997a), formed in a lagoon environment. Sample 4 is from a thin laminar bed of intertidal to supratidal stromatolite at the transition between the Kogelbeen and Gamohaan Formations (Fig. 1), which Sumner (1997a) interpreted as the shallowest depositional environment of the sequence. Samples 1, 2, and 3 represent columnar (typically irregular) stromatolites from progressively deeper settings. Most samples contain coarse-grained clear calcite cement in original cavities. Beukes (1987) and Sumner (1997a) interpreted that cement as early diagenetic marine carbonate directly precipitated from seawater or marine intraformational waters.

## 2.2. Sampling Strategy and Methods

Precambrian chemical sediments generally yield very wide ranges in recorded initial radiogenic (Sr and Nd) isotope ratios. The ranges commonly are explained in terms of detrital contamination (e.g., Derry and Jacobsen, 1990) or as artifacts of inaccurate parent decay correction owing to overprinting during diagenesis and subsequent geologic events. Hence, it is important to base sampling strategy on current knowledge regarding the effects of diagenesis on isotopic and trace element characteristics of carbonate. Experimentation with the coprecipitation of rare earth elements (REEs) and carbonate minerals has shown that most of the REE content of carbonate minerals is lattice bound with REEs substituting for $Ca^{2+}$ ions (e.g., Terakado and Masuda, 1988; Zhong and Mucci, 1995). Hence, complete dissolution of the carbonate mineral is required to mobilise large amounts of REEs and Sr from the lattice. Some of the earliest work on REE distributions in marine carbonate rocks suggested that REE patterns were not affected greatly by subsequent diagenesis (Parekh et al., 1977). Scherer and Seitz (1980) showed that aragonite coral skeletons that had been replaced by calcite during diagenesis maintained the same Yb/La ratios. However, they and Shaw and Wasserburg (1985) concluded that relatively high REE concentrations in Pleistocene and Holocene carbonates resulted from diagenetic enrichment of REEs. However, their conclusions were based on the assumption that REE concentrations of bulk limestone should reflect the REE concentration of modern skeletal carbonates. Webb and Kamber (2000) demonstrated that modern skeletal carbonates have REE concentrations orders of magnitude lower than co-occurring microbial carbonates. Hence, the relative concentration of REEs (and many other trace elements) in a noncontaminated limestone depends on the initial source of the carbonates and cannot be assumed, especially in reef settings (e.g., Scherer and Seitz, 1980) where microbialites are abundant, to be the same as for skeletal carbonates. Regardless, even the Pleistocene carbonates that Scherer and Seitz (1980) considered to have been diagenetically enriched in REEs still had basically seawater-like REE distributions.

The best constrained test of the effects of diagenesis on REE mobility in ancient limestones was conducted by Banner et al. (1988), who investigated cathodoluminescent behaviour, Sr and O isotopic ratios, Fe and Ca contents, and REE patterns of Mississippian carbonates from North America. They found that relative REE abundance and Nd isotopic ratios were not changed during extensive diagenetic alteration of marine limestones through two different phases of dolomitisation, representing two completely different diagenetic fluids and environments.

However, the same study found that cathodoluminescent behaviour and Sr and O isotopic ratios were altered, although variably, during the diagenetic events. Sr-isotope ratios remained intact in the early diagenetic dolomites, but two later generations of dolomite, which recrystalised under the influence of extraformational subsurface fluids, preserve significantly more radiogenic Sr. Schieber (1988) determined that REEs from clays were diagenetically mobilised and coprecipitated with diagenetic calcites in clay-rich limestones from the middle Proterozoic of Montana. However, REE mobilisation was only local in nature and did not affect limestones that were not directly associated with clays.

With these constraints in mind, samples for the present study were selected based on the following five criteria: (1) Microscopically visible clay and samples that were associated with shale interbeds were avoided (Sumner, 1997b); (2) preliminary acid dissolution was used to select those samples that only contained kerogen and minor $SiO_2$ as insoluble residues so as to avoid clastic detritus; (3) all samples that contain dolomite, which is a diagenetic mineral in the limestones, were avoided and samples were drilled from the same slabs from which thin sections had been made; (4) all samples lack evidence for recrystalisation, halite-bearing fluid inclusions, and secondary porosity; (5) isotopic and elemental abundances were determined on liquid aliquots from the same dissolution. It is important to recall that the Campbellrand stromatolites are essentially unmetamorphosed (Klein and Beukes, 1989) and preserve some of the finest original microstructures, which argues against significant regional diagenetic overprint and facilitates recognition of local late diagenesis.

The selected samples were drilled out of freshly cut slabs. The amount of drilled material for subsamples on which trace elements, Sr and Nd isotopes, were measured was ~1.5 g, whereas subsamples on which Nd isotopes were not determined were smaller (50–100 mg). Samples were cleaned three times in ultrapure water, dissolved in 2 M nitric acid, centrifuged, and split into two liquid aliquots. The trace element aliquot was diluted and spiked with 10 ppb internal standards (as in Webb and Kamber, 2000) for ICP-MS analysis (Table 1). Oxide levels were monitored with pure elemental solutions and appropriate interference correction was applied. Internal drift was monitored and corrected with an interleaved standard solution of known composition. The isotope aliquot was evaporated and converted to $Cl^-$ form. Sr and bulk REE were separated on cation exchange columns using standard procedures. Nd was purified on columns with HDEHP-coated inert support material. Isotope compositions of Sr and Nd were determined statically on a multicollector mass spectrometer (details given in footer of Table 2).

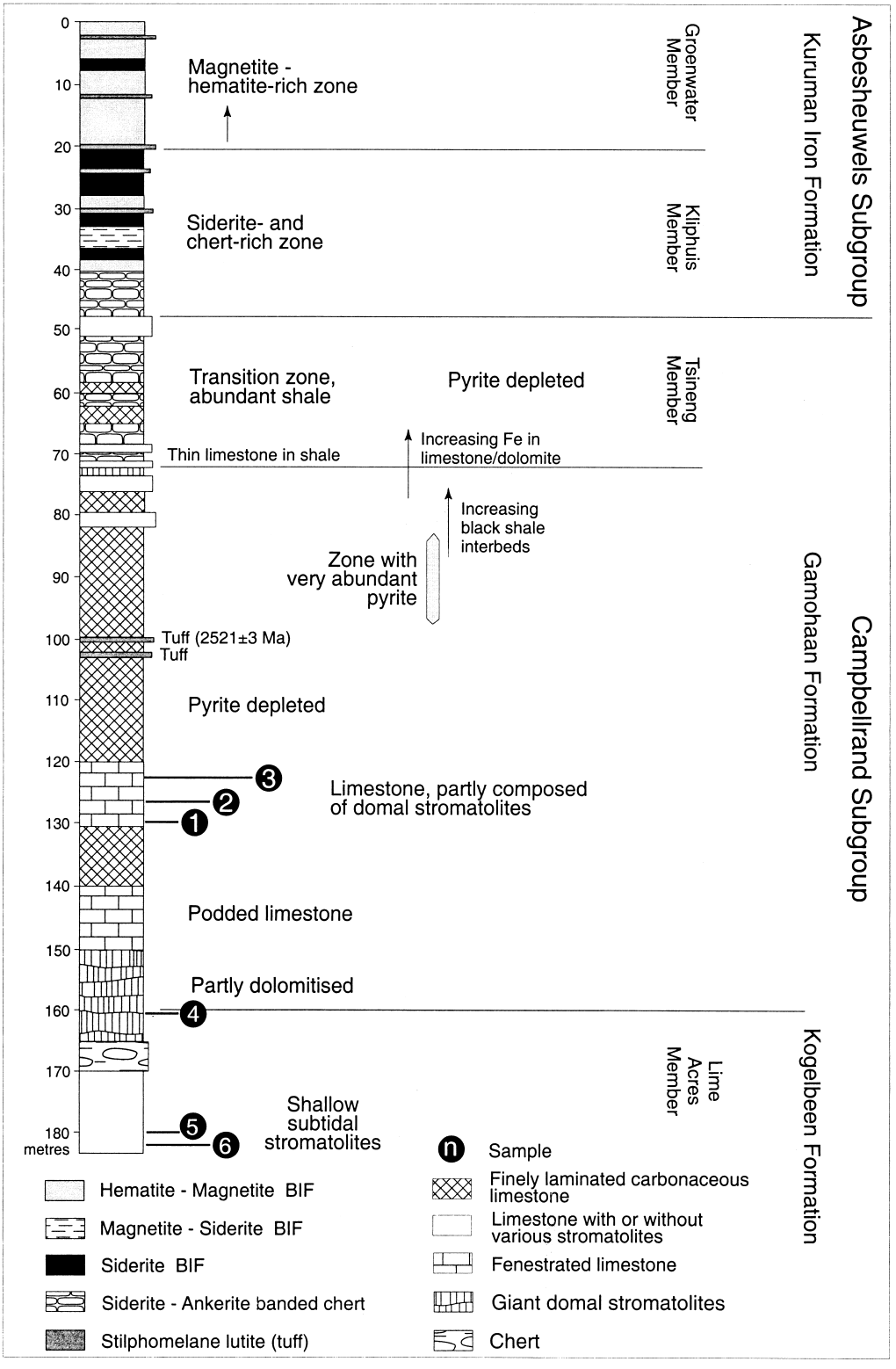


Fig. 1. Schematic lithostratigraphy of the carbonate to iron formation transition preserved in the Transvaal Supergroup, South Africa (after Beukes, 1987; Beukes pers. comm.). The tuff bed at 100 m depth was dated at 2521 ± 3 Ma by Sumner and Bowring (1996). Stromatolite samples shown by black circles.

## 3. RESULTS

### 3.1. Trace Element Data

Webb and Kamber (2000) established that microbialites incorporate REE and Y from seawater proportionally with uniform partition coefficients of $D_{REE+Y}^{microbialite/seawater} \approx 296$. However, REE concentrations in microbialites vary as a result of dilution with trapped skeletal carbonate that has lower REE and Y content. Although Sumner (1997b) found no optical evidence of trapped siliciclastic or carbonate sediment in Campbellrand stromatolites, the first point to be addressed is whether there are geochemical fingerprints of contamination from detritus and volcanic ash or of subsequent diagenesis. A useful indication of the purity of a marine carbonate sample is its recorded Y/Ho ratio. Modern seawater has an Y/Ho ratio ($>$ 44) that is substantially higher than chondrite (26–28). Elevated Y relative to Ho in seawater reflects differences in the complexation behaviour of the elements, which have identical charge and near-identical effective ionic radii (Nozaki et al., 1997). The vast majority of geologic materials (including all volcanic rocks and clastic sediments), however, have chondritic ratios (Nozaki et al., 1997). Sampled Campbellrand stromatolites, with the exception of sample 4 (Y/Ho = 26), have strongly superchondritic Y/Ho ratios of up to 101 (Fig. 2a). The average Y/Ho ratio of the 2.5 Ga stromatolites (64) is indistinguishable from that of modern Great Barrier Reef microbialites (56) and is well within the range of other modern marine proxies (44–74) (Nozaki et al., 1997).

Another indicator of uncontaminated marine REE signatures is the presence of a positive La anomaly (see Bau and Dulski, 1996) in shale-normalised REE patterns (subscript SN). A positive La anomaly is defined as an overabundance of La relative to Ce in samples that have no Ce anomaly. Because the two anomalies are related, they are best studied in a single plot that discriminates between them (Fig. 3). A comparison between modern microbialites and ancient Campbellrand microbialites reveals a clear difference. Modern microbialites possess a prominent negative Ce anomaly, namely, $(Pr/Pr^*)_{SN} > 1$, in accordance with modern shallow seawater, whereas the ancient samples have $(Pr/Pr^*)_{SN}$ indistinguishable from 1. However, both modern and ancient microbialites have significantly positive La anomalies, namely, $(Ce/Ce^*)_{SN} < 1$. The average La anomaly, expressed as $(Ce/Ce^*)_{SN}$ of the Campbellrand microbialites, is 0.76 $\pm$ 0.10, within error identical to that of modern microbialites (0.74 $\pm$ 0.02), thereby providing evidence that there is a strong marine component in the trace element inventories of the ancient limestones.

Interestingly, the Y/Ho and $(Ce/Ce^*)_{SN}$ are well correlated (Fig. 2b). At first glance, the correlation could be taken to indicate a variable degree of contamination of the carbonates by shale-like material. Mixing between the sample with the highest Y/Ho (i.e., in this interpretation, the purest sample) and PAAS (post-Archaean-Australian shale) (McLennan, 1989) results in a curve that could explain the negative correlation between Y/Ho and $(Ce/Ce^*)_{SN}$. As can be see from Figure 2b, a small degree of contamination of carbonate by shale greatly reduces the Y/Ho ratio and the La anomaly in the impure carbonate. More specifically, the Y and La anomalies would only permit a maximum of 1% contamination for all cements

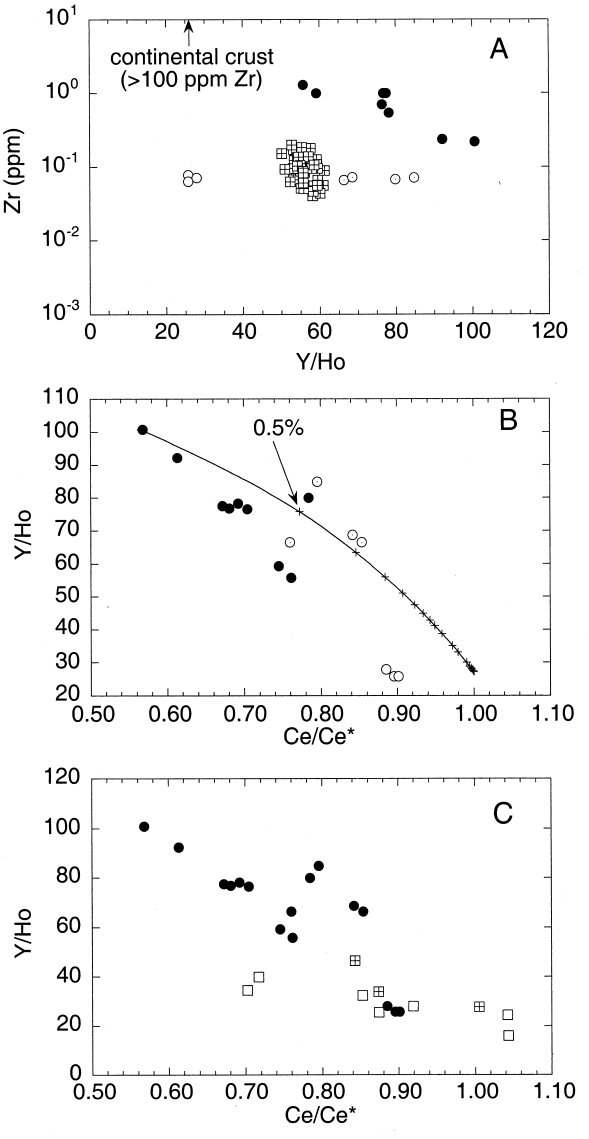


Fig. 2. (A) Plot of Y/Ho ratio vs. Zr content in 2.52 Ga microbialites. Solid circles correspond to deepest samples (1–3), open circles to shallow samples (4), and dotted circles to samples deposited in lagoons. Note that the three sample groups plot into different fields. Deep and lagoon samples have strongly superchondritic ratios, whereas shallow samples (three subsamples from sample 4) have chondritic ratios but do not show elevated Zr content. The lack of correlation between the two parameters argues against significant continental or volcanic contamination. Holocene microbialites from Heron Reef, indicated as crossed squares with data from Webb and Kamber (2000), are shown for comparison. (B) Campbellrand microbialites (same symbols as in A) show a negative correlation in Y/Ho vs. shale-normalised (PAAS; McLennan 1989) Ce/Ce* ($[Ce/0.5\ La + 0.5\ Pr]_{SN}$) space. Samples from lagoon setting and one deep subsample plot slightly above the trend. For comparison, a mixing line between the microbialite with the highest Y/Ho and shale (PAAS) is shown. Very small amounts of sediment would lead to very strongly decreased Y/Ho ratio and La anomalies. (C) Identical plot to (B) but comparing the Campbellrand carbonates (all data as solid circles) to filtered river waters from Cameroon, indicated as open squares with data from Viers et al. (1997), and filtered Japanese river (Arakawa) and estuarine (Aomi Bay) waters, indicated as crossed squares with data from Nozaki et al. (1997).

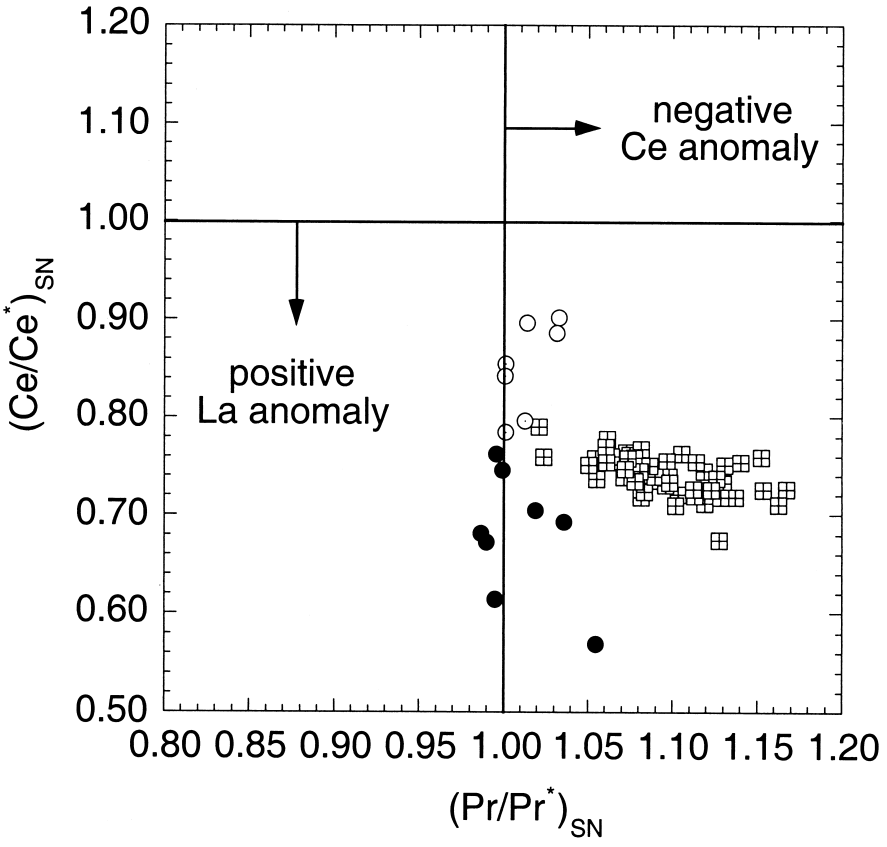


Fig. 3. Discrimination between La and Ce anomalies using a plot of shale-normalised $Pr/Pr^*$ ($[Pr/(0.5\ Ce + 0.5\ Nd]_{SN}$) vs. $Ce/Ce^*$ ($[Ce/0.5\ La + 0.5\ Pr]_{SN}$) (modified after Bau and Dulski, 1996). Same symbols as in Figure 2a. The 2.52 Ga microbialites show no Ce anomaly and have a positive La anomaly. There is a clear trend in the data, wherein the deepest samples display the strongest La anomaly. Holocene Heron Reef microbialites, indicated as crossed squares with data from Webb and Kamber (2000), share the positive La anomaly, but they also have a negative Ce anomaly consistent with that in modern well-ventilated seawater.

except sample 4. Moreover, such a small degree of contamination predicts an insignificant effect on Sr-isotope composition, which we will show below to be incompatible with the observed data. An alternative explanation for both the spread in and correlation between Y/Ho and $(Ce/Ce^*)_{SN}$ is that the samples were deposited in an environment with strongly varying dissolved REE+Y signatures. For example, modern river and estuarine waters show a range of Y/Ho and $(Ce/Ce^*)_{SN}$ compositions (Fig. 2c). REE and Y systematics in the dissolved and colloidal loads of river waters reflect those in the catchment, and because many catchments have an average composition similar to shale, the distinction between a carbonate that faithfully records such a catchment/shale signal (or the mixed signal found in estuaries or lagoons) and an open marine carbonate with minor shale contamination becomes nontrivial. Support for interpreting the REE+Y systematics of the Campbellrand stromatolites as genuine reflections of different water chemistries comes from the interpretation of the depositional environments (Sumner, 1997a) from which the samples were derived. Sample 4 formed in an intertidal to supratidal setting; samples 5 and 6 are likely to have precipitated in lagoons; samples 1, 2, and 3 represent progressively deeper facies. That trend in depositional bathymetry is consistent with water-borne REE+Y systematics (Fig. 2b), as the deeper samples have larger anomalies, which progressively weaken in the shallowest samples. The two lagoon samples tend to plot slightly off the linear trend, possibly reflecting local signatures or processes that specifically operated in the lagoon environment. Note that on Figure 2b, the lagoon samples plot closer to the modeled trend than that defined by the other samples. This is not significant, as PAAS (the shale endmember used in the model) is not likely to exactly match the composition of the true shale source. The bathymetric interpretation of the REE data is compatible with the occurrence of poorly mixed water masses (deep open ocean water, shallow shale-dominated surface water, and restricted lagoonal water) that has been suggested previously for the Campbellrand and Asbesheuwels Subgroups by Beukes et al. (1990), Bau and Dulski (1996), and Sumner (1997a).

Irrespective of the variability found in Y and La anomalies, all Campbellrand samples (with the exception of sample 4, which has a chondritic Y/Ho ratio) have reproducible and coherent REE+Y patterns (Fig. 4a) where Y is inserted into an REE plot between Dy and Ho, according to its effective ionic radius. There is a large variation in absolute concentration, which probably reflects the proportion of organic C-rich, fine-

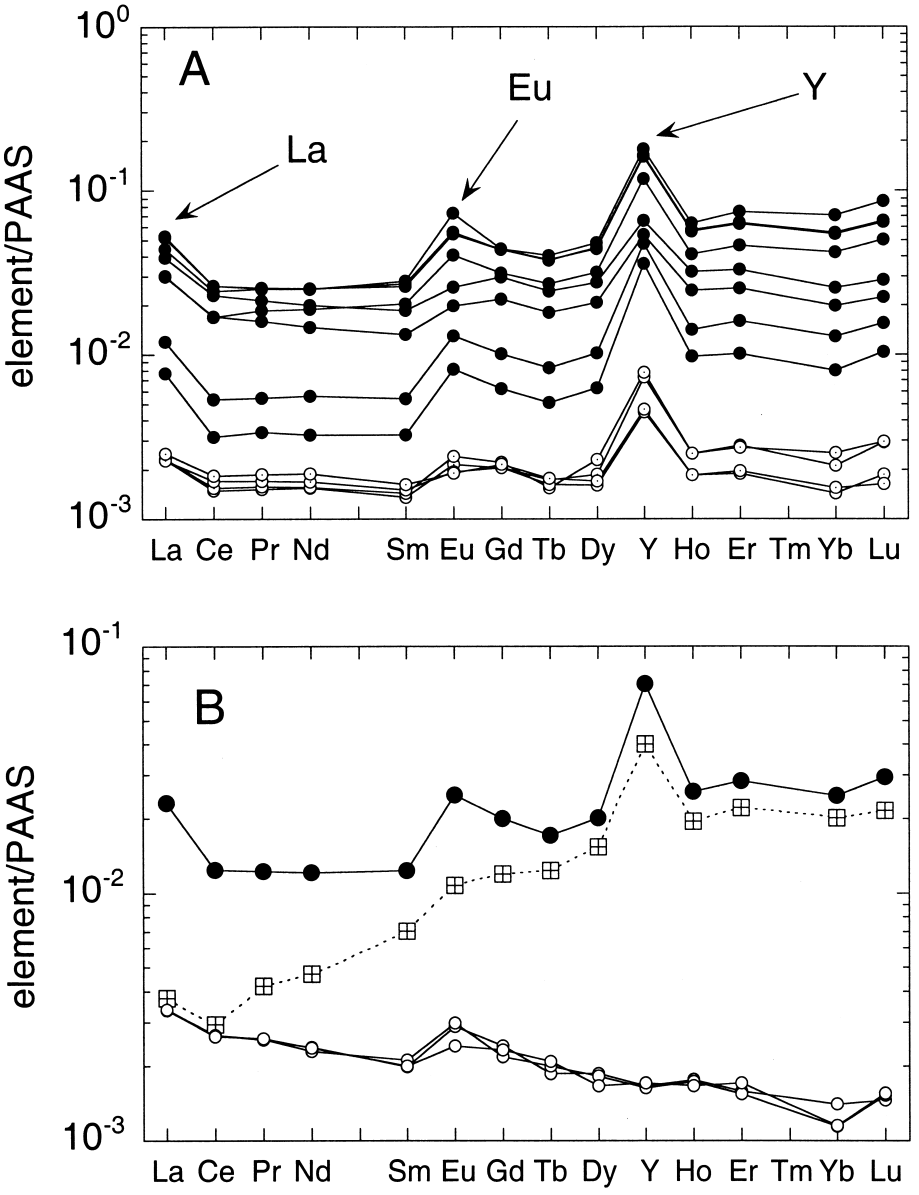


Fig. 4. PAAS normalised REE+Y plots. (A) Patterns of twelve individually drilled stromatolite subsamples (excluding sample 4) are very coherent in shape despite large differences in concentration. Note that deeper samples (solid circles) have higher total REE concentrations than lagoon samples (dotted circles). (B) Comparison of average Campbellrand microbialite (solid circles connected by solid line, excluding sample 4) with that of Holocene Heron Reef microbialites, indicated by crossed squares connected by broken line (Webb and Kamber, 2000), highlights difference in Ce and Eu anomalies and the degree of LREE depletion, while still confirming the similarity in the general marine aspect (e.g., Y and La anomalies). The shallowest Campbellrand microbialites (sample 4: small open circles connected by solid lines) have consistently different patterns.

grained laminated stromatolitic calcite to organic C-free, coarse-grained void-filling cement, e.g., compare subsamples 3a and 3b, which are dominated by coarse cement, with 3c and 3d, which were drilled from laminated precipitates (Table 1). That could imply an affinity of REE (and other elements such as U, Pb, Cs, and Rb) for the organic biofilms of microbialites. Alternatively, the difference in REE content could have a kinetic causality, as the clear, organic C-poor calcite is much coarser grained, implying faster growth. Regardless, the most important observation is that the REE+Y patterns are independent of concentration. That independence is significant because it confirms that the latest precipitates (the coarse-grained calcite cements) were in equilibrium with pore waters, which essentially had seawater chemistry.

Correlation of the Y and La anomalies with interpreted depositional bathymetry, combined with the sensitivity of the anomalies to clastic contamination, suggests that the REE systematics of the studied carbonates, with the possible exception

Table 1. Trace element contents of 15 stromatolitic carbonates from the 2.52 Ga Campbellrand platform.

| Sample # | 1 | | 2 | | 3 | | | | 4 | | | 5 | | 6 | |
|---|---|---|---|---|---|---|---|---|---|---|---|---|---|---|---|
| Formation | Gamohaan | | Gamohaan | | Gamohaan | | | | Kogelbeen | | | Kogelbeen | | Kogelbeen | |
| Structure | Conophytic stromatolite & contorted algal mats | | Conophytic stromatolite | | Conophytic stromatolite | | | | Laminar stromatolite | | | Laminar stromatolite | | Laminar stromatolite | |
| Subsample | a | b | a | b | a | b | c | d | a | b | c | a | b | a | b |
| Proportion of late calcite fills | ≈10% | ≈15% | 0% | 0% | ≈80% | ≈80% | ≈20% | ≈20% | ≈50% | ≈50% | ≈50% | ≈0% | ≈0% | ≈25% | ≈25% |
| Sr | 37252 | 28932 | 41062 | 40815 | 39744 | 42272 | 47063 | 41733 | 41853 | 38219 | 37214 | 23857 | 23679 | 30751 | 27851 |
| Rb | 7.5 | 9.2 | 342 | 320 | 3.0 | 6.4 | 275 | 159 | 38.3 | 41.9 | 42.6 | 12.2 | 14.6 | 25.2 | 24.5 |
| Y | 1774 | 1450 | 4309 | 4410 | 972 | 1290 | 3179 | 4793 | 44.9 | 44.1 | 46.0 | 197 | 211 | 121 | 126 |
| Zr | 1289 | 989 | 993 | 991 | 217 | 233 | 533 | 695 | 77.6 | 63.2 | 70.7 | 67.6 | 71.1 | 66.1 | 72.3 |
| Nb | 6.9 | 3.0 | 15.8 | 15.2 | 5.0 | 3.4 | 7.3 | 3.9 | 2.9 | 2.3 | 3.5 | 2.1 | 1.7 | 3.0 | 2.5 |
| Cs | 2.3 | 2.9 | 33.8 | 31.6 | 1.0 | 0.8 | 28.8 | 18.7 | 7.8 | 8.8 | 7.7 | 3.9 | 4.8 | 4.6 | 4.0 |
| Ba | 597 | 432 | 5010 | 4972 | 2912 | 3920 | 6051 | 5313 | 6143 | 5465 | 5396 | 3584 | 3954 | 5379 | 5217 |
| La | 1491 | 1148 | 1973 | 2015 | 294 | 457 | 1157 | 1682 | 129 | 128 | 129 | 87.2 | 88.7 | 86.9 | 95.5 |
| Ce | 1835 | 1364 | 2090 | 2098 | 250 | 425 | 1346 | 1942 | 211 | 212 | 210 | 119 | 123 | 135 | 146 |
| Pr | 190 | 141 | 225 | 226 | 29.8 | 48.1 | 164 | 223 | 22.5 | 22.6 | 22.8 | 13.4 | 13.9 | 15.0 | 16.4 |
| Nd | 682 | 500 | 858 | 863 | 110 | 190 | 641 | 852 | 80.8 | 77.4 | 80.2 | 52.2 | 52.8 | 57.2 | 63.6 |
| Sm | 104 | 73.5 | 150 | 145 | 18.0 | 29.8 | 114 | 156 | 11.0 | 11.7 | 11.1 | 7.5 | 8.0 | 8.3 | 9.0 |
| Eu | 28.0 | 21.4 | 60.7 | 58.8 | 8.8 | 14.1 | 43.7 | 78.3 | 3.1 | 3.2 | 2.6 | 2.3 | 2.6 | 2.1 | 2.0 |
| Gd | 139 | 102 | 204 | 205 | 29.0 | 47.0 | 147 | 207 | 11.2 | 10.2 | 10.8 | 9.6 | 10.3 | 9.5 | 10.0 |
| Tb | 18.9 | 14.0 | 29.5 | 29.3 | 3.9 | 6.4 | 21.0 | 31.1 | 1.4 | 1.5 | 1.6 | 1.3 | 1.2 | 1.2 | 1.4 |
| Dy | 129 | 97.7 | 207 | 211 | 29.4 | 47.8 | 149 | 226 | 8.7 | 8.5 | 7.8 | 8.7 | 10.7 | 7.5 | 7.9 |
| Ho | 31.9 | 24.5 | 56.2 | 56.9 | 9.7 | 14.0 | 40.7 | 62.7 | 1.7 | 1.7 | 1.6 | 2.5 | 2.5 | 1.8 | 1.8 |
| Er | 94.2 | 72.5 | 179 | 181 | 28.8 | 45.8 | 132 | 212 | 4.5 | 4.4 | 4.9 | 8.0 | 7.7 | 5.4 | 5.6 |
| Yb | 72.6 | 56.2 | 153 | 156 | 22.6 | 36.3 | 119 | 199 | 4.0 | 3.2 | 3.2 | 5.9 | 7.1 | 4.0 | 4.4 |
| Lu | 12.4 | 9.7 | 28.0 | 28.5 | 4.5 | 6.7 | 21.8 | 37.2 | 0.6 | 0.7 | 0.7 | 1.3 | 1.3 | 0.8 | 0.7 |
| Hf | 8.7 | 8.1 | 16.5 | 15.9 | 3.9 | 3.0 | 14.7 | 13.3 | 2.4 | 2.1 | 2.0 | 1.3 | 1.9 | 1.8 | 1.3 |
| Pb | 31.1 | 30.8 | 765 | 758 | 101 | 194 | 556 | 493 | 183 | 182 | 222 | 290 | 589 | 276 | 473 |
| Th | 3.8 | 2.3 | 59.1 | 52.7 | 1.5 | 2.0 | 102 | 72.1 | 20.8 | 18.6 | 18.0 | 15.1 | 17.6 | 15.5 | 17.4 |
| U | 2.0 | 5.3 | 102 | 109 | 4.1 | 7.8 | 80.1 | 87.6 | 11.8 | 11.2 | 10.9 | 22.9 | 24.2 | 24.0 | 22.5 |

All concentrations in parts per billion (ppb). Precision was 4–6% for abundances $>$ 10 ppb and $\leq$ 10% for the most depleted elements.

of sample 4, represent proxies for the waters from which they precipitated. Sample 4 has a chondritic Y/Ho ratio and the weakest La anomaly. Because it has very low total REE abundance, the possibility of clastic contamination in this sample cannot be ruled out. In the following discussion of further features of REE systematics, we assume that the remaining samples are free from significant contamination.

The Campbellrand stromatolite REE+Y patterns have three features that set them apart from those of modern microbialites: (1) reduced light-to-heavy REE fractionation, (2) an absence of negative Ce anomaly, and (3) the presence of positive Eu anomaly. The absence of a negative Ce anomaly is most accurately expressed in the average $(Pr/Pr^*)_{SN}$ ratio of unity ($1.008 \pm 0.020$, excluding sample 4). The absence of a negative Ce anomaly in the Campbellrand microbialites is consistent with REE systematics in the immediately overlying Kuruman iron formation and the correlative Penge iron formation (Bau and Dulski, 1996), thereby reinforcing the view that at 2.52 Ga, the waters from which the Campbellrand carbonates precipitated were not sufficiently oxidising to allow formation of less soluble or more reactive Ce(IV) species. Sr-isotope compositions discussed below indicate that at least some of the carbonates are open marine, which suggests that late Archaean/earliest Proterozoic oceans were anoxic, which is in agreement with other evidence (see, e.g., Collerson and Kamber, 1999; Canfield et al., 2000; Farquhar et al., 2000).

Compared to modern microbialites, Campbellrand samples are less depleted in light REE (LREE) (Fig. 4b). The REE+Y pattern of modern marine water reflects the residual inventory after preferential extraction of LREE in estuaries (mainly during coagulation of colloids by sea salts) and further preferential LREE removal by adsorptive scavenging. Therefore, the signature recorded by Campbellrand stromatolites appears to reflect waters that were less affected by coagulation and adsorptive scavenging. Hence, the La and Y anomalies, which are believed to be caused by similar processes, should be correlated with relative LREE depletion. Indeed, a strong correlation exists between LREE depletion, expressed as $(Sm/Yb)_{SN}$, and the extent of the La anomaly: $(Ce/Ce^*)_{SN}$ (Fig. 5a). Importantly, contamination with shale-like material (or other detritus) can be excluded as an alternative explanation, because it would effectively obliterate the positive La anomaly. Average shallow marine seawater (as recorded by Great Barrier Reef microbialites) is somewhat more strongly depleted in LREE than the waters from which the Campbellrand stromatolites precipitated. However, the relatively high $(Ce/Ce^*)_{SN}$ of modern microbialites is partly the result of a true negative Ce anomaly, which the ancient samples lack. In summary, the variability in LREE

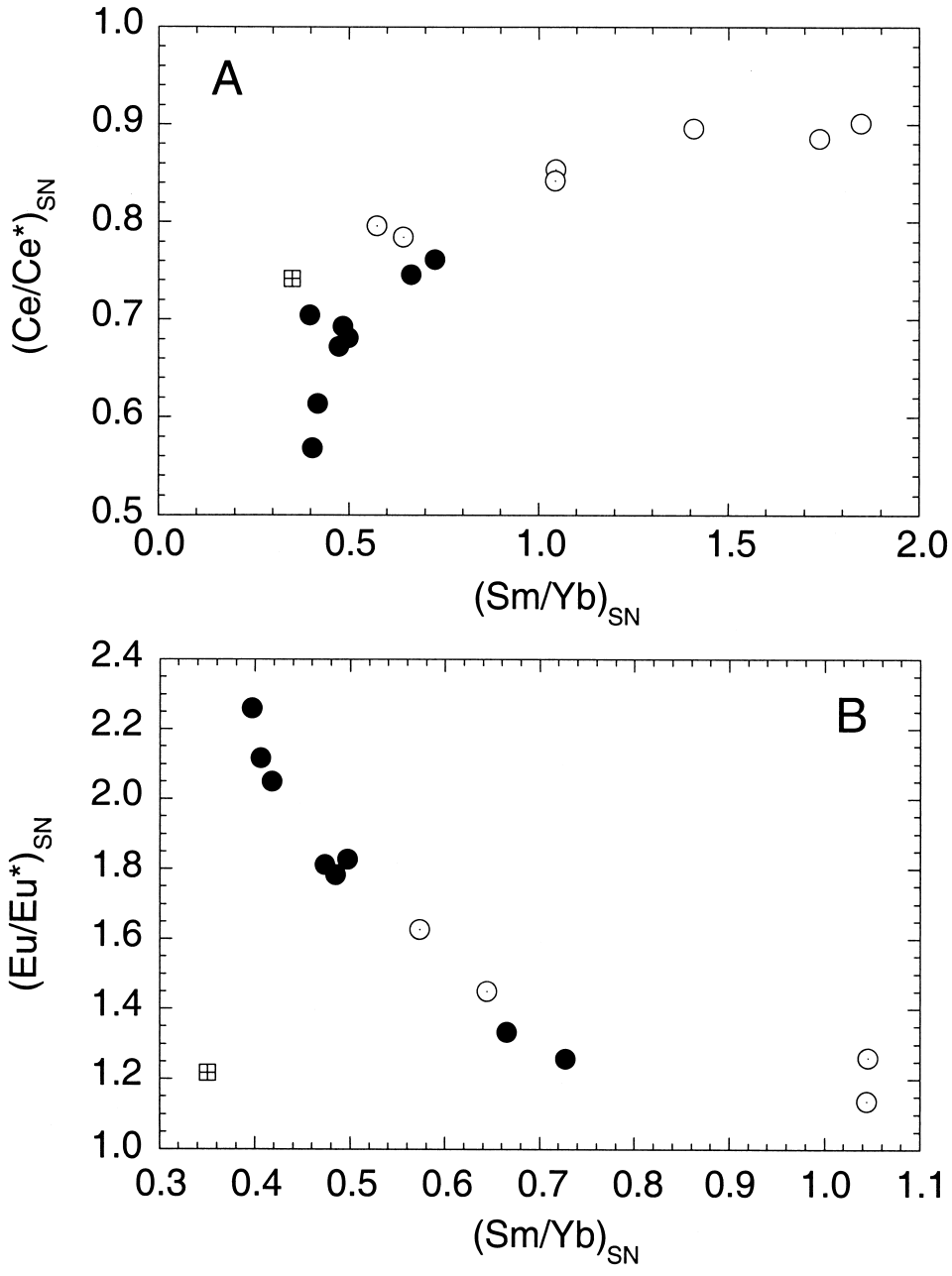


Fig. 5. (A) Campbellrand microbialites show a strong correlation between LREE depletion (expressed as $(Sm/Yb)_{SN}$) and the extent of the La anomaly ($(Ce/Ce^*)_{SN}$). The deepest samples (solid circles) show the strongest LREE depletion, followed by the lagoon samples (dotted circles), whereas the shallowest samples (open circles) are LREE-enriched relative to shale, possibly indicating local erosion of more evolved continental material (see also Fig. 4b). The average Holocene Heron Reef microbialite (crossed square) is plotted for comparison. (B) Campbellrand stromatolites (same symbols as in A, sample 4 omitted) also show a good correlation between LREE depletion (expressed as $(Sm/Yb)_{SN}$) and the extent of the Eu anomaly ($(Eu/Eu^*)_{SN}$). Note that although Holocene microbialites (crossed square) and modern seawater also have a slight positive Eu anomaly, their extent does not compare with that recorded by the 2.52 Ga samples.

depletion is coupled to the La and Y anomalies, and all reflect a transition between open marine and estuarine waters.

The most important feature of the Campbellrand stromatolite REE+Y systematics is the presence of a positive Eu anomaly (Fig. 4a,b). Positive Eu anomalies have been reported previously for early Precambrian chemical sediments (e.g., Derry and Jacobsen, 1990; Danielson et al., 1992; Bau and Möller, 1993; Alibert and McCulloch, 1993), particularly in banded-iron formation (BIF). A positive Eu anomaly cannot be caused directly by the redox state of seawater. Derry and Jacobsen (1990) and Danielson et al. (1992) demonstrated that the most likely origin of a marine positive Eu anomaly is increased

Table 2. Sr- and Nd-isotope data.

| Sample | Sub-sample | Rb (ppm) | Sr (ppm) | $^{87}Rb/^{86}Sr$ | Sm (ppm) | Nd (ppm) | $^{147}Sm/^{144}Nd$ | $^{87}Sr/^{86}Sr$ | $^{87}Sr/^{86}Sr$ initial | ± | $^{143}Nd/^{144}Nd$ | ± | $^{143}Nd/^{144}Nd$ initial | εNd (2.52 Ga) | ± |
|---|---|---|---|---|---|---|---|---|---|---|---|---|---|---|---|
| 1 | a | 0.008 | 37.3 | 0.0006 | 0.104 | 0.682 | 0.0922 | 0.702443 | 0.702422 | 08 | 0.510983 | 12 | 0.509450 | 1.61 | 0.53 |
| 1 | b | 0.009 | 28.9 | 0.0009 | 0.074 | 0.500 | 0.0895 | 0.702503 | 0.702470 | 09 | 0.510961 | 09 | 0.509473 | 2.06 | 0.46 |
| 2 | a | 0.342 | 41.1 | 0.0235 | 0.150 | 0.858 | 0.1057 | 0.704860 | 0.704003 | 17 | 0.510943 | 20 | 0.509186 | −3.58 | 0.74 |
| 2 | b | 0.320 | 40.8 | 0.0222 | | | | 0.704677 | 0.703870 | 16 | | | | | |
| 3 | a | 0.003 | 39.7 | 0.0002 | 0.018 | 0.110 | 0.0989 | 0.702298 | 0.702290 | 10 | 0.511039 | 22 | 0.509394 | 0.51 | 0.75 |
| 3 | b | 0.006 | 42.3 | 0.0004 | 0.030 | 0.190 | 0.0955 | 0.702377 | 0.702362 | 08 | 0.511043 | 19 | 0.509456 | 1.72 | 0.68 |
| 3 | c | 0.275 | 47.1 | 0.0165 | | | | 0.704244 | 0.703643 | 14 | | | | | |
| 3 | d | 0.159 | 41.7 | 0.0107 | 0.156 | 0.852 | 0.1107 | 0.704088 | 0.703696 | 13 | 0.511190 | 11 | 0.509349 | −0.37 | 0.57 |
| 4 | a | 0.038 | 41.9 | 0.0026 | | | | 0.703443 | 0.703349 | 10 | | | | | |
| 4 | b | 0.042 | 38.2 | 0.0031 | 0.012 | 0.077 | 0.0942 | 0.703632 | 0.703519 | 10 | 0.510930 | 21 | 0.509363 | −0.09 | 0.72 |
| 4 | c | 0.043 | 37.2 | 0.0032 | | | | 0.703607 | 0.703489 | 08 | | | | | |
| 5 | a | 0.012 | 23.9 | 0.0014 | | | | 0.704229 | 0.704176 | 11 | | | | | |
| 5 | b | 0.015 | 23.7 | 0.0017 | 0.008 | 0.053 | 0.0913 | 0.704603 | 0.704539 | 11 | 0.510906 | 23 | 0.509388 | 0.40 | 0.75 |
| 6 | a | 0.025 | 30.8 | 0.0023 | | | | 0.703980 | 0.703896 | 09 | | | | | |
| 6 | b | 0.025 | 27.9 | 0.0025 | 0.009 | 0.064 | 0.0850 | 0.705007 | 0.704917 | 09 | 0.510555 | 27 | 0.509142 | −4.44 | 0.80 |

Errors on measured isotope ratios are two sigma absolute and refer to the last two digits of the reported ratios. Errors on initial ratios also include a propagated 1% uncertainty on the parent/daughter ratio (calculated from ICP-MS analysis of a liquid aliquot).

Repeat analyses of NBS SRM 987 Sr and La Jolla Nd standards yielded $^{87}Sr/^{86}Sr$ 0.710255 ± 16 and $^{143}Nd/^{144}Nd$ 0.511861 ± 12, respectively. $\varepsilon_{Nd}$ calculated relative to chondritic initial $^{143}Nd/^{144}Nd$ of 0.512638 and $^{147}Sm/^{144}Nd$ of 0.1967.

oceanic input of relatively hot hydrothermal fluids emanated at midocean ridges. The existence of such an anomaly in relatively shallow seawater suggests that the balance between hydrothermal and erosional inputs was dramatically different (i.e., reversed) from today. Documentation of a positive Eu anomaly requires that two major problems be overcome. First, the possibility exists that the anomaly could be an artifact of the chosen normalisation (in our case of PAAS). However, whereas modern seawater has a slight positive Eu anomaly relative to PAAS (Fig. 5b), the anomaly does not compare in magnitude with anomalies documented in BIF and in Campbellrand carbonates. Second, in many documented cases, the Eu anomaly appears to be rather variable and variation does not seem to be systematic with other geochemical indicators. One cause for the variable Eu anomaly is the slight positive Gd anomaly in seawater. Indeed, even modern microbialites have a slight positive Gd anomaly (Webb and Kamber, 2000), and the Eu anomaly $(Eu/Eu^*)_{SN}$ should therefore be expressed as (Eu/[2/3Sm + 1/3Tb]). Regardless, the main problem with previously existing evidence for a positive Eu anomaly in early Precambrian oceans is the lack of correlation between the anomaly and other geochemical parameters. For example, Bau and Dulski (1996) commented on the lack of correlation with Sm/Yb, concluding that BIF microbands with high $(Eu/Eu^*)_{SN}$ correspond to upwelling events of deepwater masses with a strong hydrothermal signal. In Campbellrand stromatolites, however, the Eu anomaly correlates very well with the previously discussed REE+Y patterns. For example, a very good negative correlation exists between the Eu anomaly and the Sm/Yb ratio (Fig. 5b). The coherent behaviour of REE+Y is best explained if the various Campbellrand stromatolites precipitated from waters with different chemistries (i.e., the deepest, most marine sample has the highest Y/Ho, the lowest Sm/Yb, and the most prominent La and Eu anomalies).

### 3.2. Isotope Data

Sr-isotope data for all subsamples and Nd-isotope data for a selection of samples are presented in Table 2 and illustrated in Figures 6 and 7.

Initial $^{87}Sr/^{86}Sr$ ratios for all carbonate samples are compared to an estimate of coeval depleted mantle and to the least radiogenic Sr recorded in some late- to mid-Archaean carbonates (Fig. 6a). The least radiogenic Sr commonly has been assumed to represent the most reasonable estimate of that of open ocean waters (e.g., Mirota and Veizer, 1994). If that assumption is correct, the average of the four least radiogenic Campbellrand stromatolites yields a $^{87}Sr/^{86}Sr$ ratio of 0.702386 ± 78 as the best approximation of Sr-isotope composition of 2.52 Ga oceans. That value plots along the roughly linear trend defined by other Archaean proxies (Fig. 6a), which suggests that marine Sr was only marginally more radiogenic than coeval mantle. However, it is clear that the total range of Sr-isotope compositions in Campbellrand stromatolites (and in Archaean limestones and barite determined in other studies) by far exceeds possible temporal fluctuations in the open ocean.

The wide range in recorded initial Sr-isotope ratios has been used to argue that the samples with radiogenic values were affected by detrital contamination or subsequent diagenesis. However, for the Campbellrand carbonates, that possibility can be evaluated and rejected using simple binary mixing models. As shown previously (Fig. 2b), the positive marine La anomaly is a very sensitive indicator of contamination. Very small degrees of shale contamination effectively eradicate an La anomaly or other marine features of the REE+Y patterns, such as the Y/Ho or $(Eu/Eu^*)_{SN}$ ratios, owing to the disparity in REE+Y concentration between shale (relatively high) and carbonate (very low). Indeed, a hypothetical mixing curve between a clean carbonate and shale has a strongly hyperbolical shape in Sr isotope vs. La anomaly space (Fig. 7). All Campbellrand carbonates with $^{87}Sr/^{86}Sr > 0.703$ plot clearly above that mixing line. In other words, the amount of contamination required to explain their Sr-isotope ratios would effectively mask any La anomaly (the effect is stronger for less radiogenic contaminants). The only stromatolite samples that could be slightly contaminated are those with $^{87}Sr/^{86}Sr < 0.703$, because they have variable La anomalies but almost constant

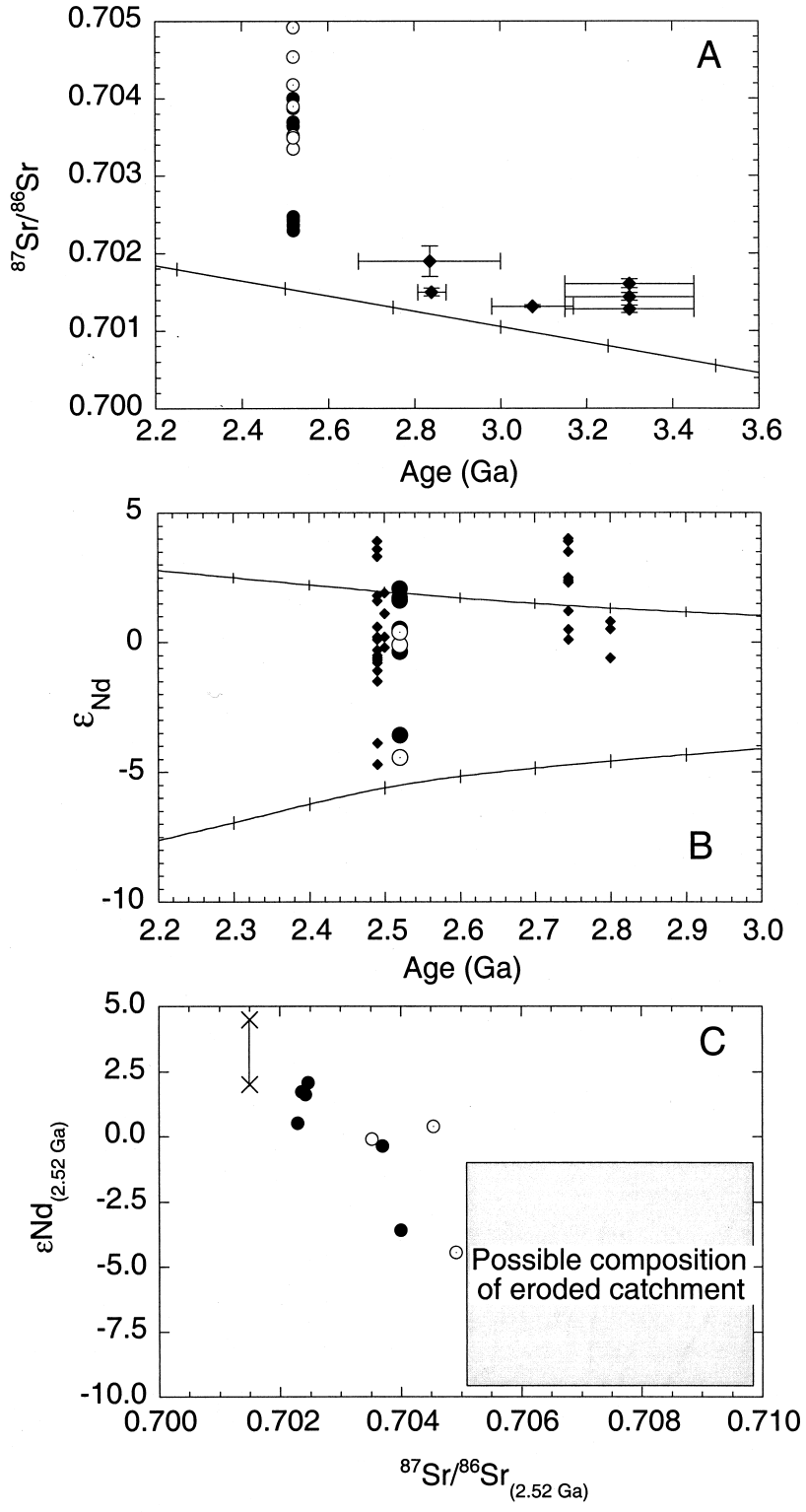


Fig. 6. Isotope plots. (A) Initial $^{87}Sr/^{86}Sr$ ratios of marine proxies vs. age. Campbellrand stromatolites are plotted as solid circles (deep samples), open circles (shallow samples), and dotted circles (lagoon samples). For comparison, estimates of late- to mid-Archaean limestones and barites from the literature are shown (only least radiogenic data plotted). Data points (diamond symbols with age error bars): 2.835 ± 185 Ga is Steep Rock Group carbonate from Canada (Sr data from Veizer and Compston, 1976 with age information from Wilks and Nisbet, 1988); 2.839 ± 33 Ga is Bulawayan limestone from Zimbabwe (Sr data from Veizer and Compston, 1976 with age data from Moorbath et al., 1987); 3.075 ± 95 Ga is average of marble in Ramagiri schist belt from India (Zachariah, 1998); 3.300 ± 150 Ga are compositions of three stratiform barite

Sr-isotope ratios. Similar results were obtained when modeling Sr isotopes vs. Y/Ho and La/Sm. In summary, although a general trend exists toward smaller La anomalies with more radiogenic Sr, it cannot reflect contamination and, therefore, requires a different explanation.

The remaining explanation for the wide range in initial Sr-isotope ratios is that they reflect dissolved Sr in the waters from which the carbonates precipitated. Because late diagenesis and overprint is relatively easily recognised on the basis of mineralogy (dolomite vs. calcite), and because dolomite-bearing samples were strictly avoided in sampling, observed Sr-isotope ratios can only reflect seawater or early diagenetic fluids. Furthermore, it is important to point out that the Campbellrand carbonate platform is several hundred to 1500 m thick and constitutes a considerable blanket, which would have isolated samples in the upper part of the stratigraphy (e.g., those used in this study) from potential hydrothermal radiogenic Sr sources originating in the buried crystalline Kaapvaal basement. Therefore, the recorded Sr-isotope ratios could only reflect true marine waters or early diagenetic waters. The former explanation, discussed in more detail in sections 4.2 and 4.3, would require the existence of ill-mixed water bodies with different Sr-isotope compositions (as also indicated by certain REE aspects). The second explanation would require the existence of sufficient sources of radiogenic Sr from within the stratigraphy. That appears questionable, not only because interbedded shale beds are very rare and volumetrically insignificant in the succession, but also because shale Sr contents are lower (Klein and Beukes, 1989) than those of the carbonates. If sufficient shale-derived Sr existed to strongly affect Sr-isotope ratios, seawater-like REE distributions could not be retained, as shale has a higher total REE to Sr ratio than carbonate. Furthermore, the coarse-grained calcite cements in fenestrae, which Sumner (1997a) regards as possibly early diagenetic products, have less radiogenic Sr than coexisting organic C-rich fine-grained calcite, which are interpreted as direct seawater precipitates (i.e., samples 3a and 3b vs. 3c and 3d shown in Table 1). Last, because Sr appears to be more fluid mobile than Nd during diagenesis (Banner et al., 1988), a correlation between Nd- and Sr-isotope ratios (as shown in Fig. 6c and discussed below) argues against a diagenetic origin of the more radiogenic Sr (and Nd).

A plot for Nd-isotope data vs. age is given in Figure 6b. The Campbellrand stromatolites have a narrow range in $^{147}Sm/^{144}Nd$ ratio (0.0895–0.1057), but record a rather wide range in Nd-isotope compositions (Table 2). No significant correlation was found between $^{147}Sm/^{144}Nd$ and $^{143}Nd/^{144}Nd$ ratios, so that the calculated initial Nd-isotope ratios range between −4.4 and +2.1 $\varepsilon_{Nd}$ (Fig. 6b). The range encompasses almost the entire variation expected for 2.52 Ga input sources (i.e., from mantle values to typical continent-derived sediment). The range in Nd-isotope initial ratios is similar to that observed in previous studies of chemical sediments of similar age (Fig. 6b) and requires an explanation similar to the Sr isotopes. However, owing to the stability of REE in calcite, even after severe diagenesis and dolomitisation (Banner et al., 1988), Nd-isotope compositions of our well-preserved carbonates are interpreted as reflecting those of ocean water rather than extra-formational or later diagenetic fluids. The observed correlation of Sr- and Nd-isotope variation (Fig. 6c) is robust, because our Sr- and Nd-isotope data were obtained from liquid aliquots from which we also determined trace element composition. There is a linear trend with negative slope from mantle-like isotope composition toward more crustal values. The significance of that finding is that it demonstrates for the first time that radiogenic Nd-isotope compositions recorded by ancient chemical sediments are not simply artifacts of inappropriate Sm-decay correction. Disturbance of the Sm-Nd system during postdiagenetic overprint could only lead fortuitously to the correlation between Sr and Nd isotopes. Therefore, at the very least, we argue that the mantle-like isotope compositions are true reflections of the waters from which the stromatolites precipitated.

We suggest that the variations in trace element and isotope ratios reflect, to a first approximation, those of the waters from which the carbonates precipitated, and that the carbonates were deposited in an environment where waters with different chemistries mixed. The observed scatter around ideal mixing curves is likely the result of differences in conservation behaviour of the compared elements, minor contamination (by which Sr is less affected than the REE), and temporal changes in the isotope and REE compositions of the endmember waters. Furthermore, residence times of elements in mixing water bodies (possibly with very different degrees of oxygenation) are unknown. For example, the low Sr content of all Archaean carbonates could imply a lower Sr content in Archaean seawater and hence a shorter residence time (and by implication, a higher provinciality) of Sr in seawater.

Fig. 6. (Continued) beds from Ghattihosahalli, India (Deb et al., 1991). Note that the least radiogenic data points define an array that is roughly parallel to the estimated depleted mantle evolution curve (solid line, calculated using a primordial $^{87}Sr/^{86}Sr$ ratio of 0.6995 and a $^{87}Rb/^{86}Sr$ ratio of 0.07). (B) Initial Nd isotope composition (expressed in $\varepsilon$ notation) vs. age. Campbellrand stromatolites plotted as same symbols as in A. For comparison, data are plotted for BIF (diamond symbols) from the Gamohaan and Penge formations, South Africa (data from Bau et al., 1997b), from Michipicoten, Canada (data from Jacobsen and Pimentel-Klose, 1988), from the Malene supracrustals, Greenland (data from Shimizu et al., 1990), and from Hamersley, Australia (data from Miller and O'Nions, 1985 and Jacobsen and Pimentel-Klose, 1988). Also plotted are evolution lines for the MORB-source mantle (upper line) and an estimated erosion mix (lower line) from Nägler and Kramers (1998). (C) Campbellrand stromatolites (same symbols as in A) define a linear array with negative slope in a plot of $^{87}Sr/^{86}Sr$ ratio vs. initial $\varepsilon_{Nd}$. The most juvenile samples plot very close to the composition estimated for MORB-source mantle (crosses connected by solid line, encompassing linear and S-shaped Nd-isotope mantle evolutions at 2.52 Ga). Those samples with more radiogenic Sr generally have less radiogenic Nd and the linear array points to the area in Sr-Nd space thought to have been occupied by 2.52 Ga Kaapvaal craton erodible crust (gray shaded box: Nd-isotope estimate from Jahn and Condie, 1995; Sr-isotope composition estimated based on 0.4–1.0 Ga crustal residence time before erosion).

## 4. DISCUSSION

### 4.1. Implications for Oxygenation State of the Late Archaean Ocean and Atmosphere

Ce is the only REE that may be oxidised in natural environments and is thus directly sensitive to changes in the redox conditions of seawater. Modern oxidised seawater shows a negative Ce anomaly with respect to the strictly trivalent REE, because Ce(IV) is less soluble in seawater and more easily adsorbed onto particles (mainly FeMn-oxyhydroxides). Modern marine microbialites show a negative Ce anomaly, but Webb and Kamber (2000) found that the extent of the anomaly might not strictly reflect that of surrounding waters, because the Ce concentration of very shallow seawater is highly variable (although generally indicative of a negative anomaly) and difficult to quantify by a proxy. Regardless, the absence of a negative Ce anomaly in the 2.52 Ga Campbellrand microbialites (Fig. 3) in itself is strong but insufficient evidence for deposition in anoxic waters.

All REE are indirectly sensitive to redox conditions in the hydrosphere, as demonstrated by their abundances along transects from oxygenated waters into deep, isolated anoxic basins where REE redox cycling occurs above the chemocline (German et al., 1991). REE redox cycling is a reflection of Fe-Mn redox cycling, because FeMn-oxyhydroxide particle reactivity of the trivalent REE is high but changes as a function of ionic ratio and electron configuration (Bau, 1999). Dissolution of FeMn-oxyhydroxides in anoxic waters can cause REE patterns complementary to those of the overlying oxygenated water column (e.g., Bau et al., 1997a). The high FeMn-oxyhydroxide particle reactivity of the LREE is the main cause for the inferred low input of Nd to the present marine inventory. Above modern submarine vents, fluids with REE patterns very different from seawater are emanated and mix with ambient seawater, leading to Fe oxidation and REE coprecipitation. Mitra et al. (1994) suggested that hydrothermal input to the oceans could lead to a net depletion of total REE as a consequence of Fe scavenging. However, in an anoxic deep ocean, dissolved Fe(II) would not precipitate as oxyhydroxide and would have no scavenging effect on REE. Two aspects of the Campbellrand carbonates reinforce previous claims for a stronger hydrothermal oceanic input (and hence, largely anoxic deep seas). First, there is a strong positive Eu anomaly (relative to shale). It is now widely agreed that hot hydrothermal vent waters are by far the most likely source for such an anomaly, as documented from many modern ridges (e.g., Edmond et al., 1979; Michard and Albarède, 1986; Mitra et al., 1994). Positive Eu anomalies in BIF have long been attributed to hydrothermal oceanic input and are widely documented (e.g., Fryer et al., 1979; Derry and Jacobsen, 1990; Danielson et al., 1992; Bau and Möller, 1993). Second, there is the primitive Nd-isotope composition. Variations in Sr- and Nd-isotope ratios in the Campbellrand carbonates are correlated. The most primitive isotope ratios recorded in the carbonates approach those of coeval MORB-source mantle. Such isotope ratios are additional evidence for a strong hydrothermal REE input into 2.52 Ga oceans.

We emphasise that our findings do not necessarily imply that carbonate deposition itself occurred in anoxic waters. Carbonate precipitation can be induced in modern microbialite communities by a variety of autotrophic or heterophil metabolic processes that occur in aerobic or anaerobic conditions, in ambient waters, or in protected microenvironments (e.g., Castanier et al., 1999). Campbellrand stromatolites were precipitated largely at shallow platform depths, which would be consistent with aerobic, photosynthetic autotrophs such as marine cyanobacteria. The large variation in elemental and isotopic ratios of the carbonates further indicates that the site of deposition was characterised by the mixing of deep ocean waters and continent-derived (meteoric or epicontinental sea) waters. The significant feature is the survival of the positive Eu anomaly and primitive Nd-isotope signatures from hydrothermal input into the deep ocean as fingerprints, although diluted, on the very shallow carbonate platform, because large scale advection of hydrothermal Nd is only possible in an anoxic ocean.

### 4.2. Implications of Continental Chemical and Isotopic Signatures

Sedimentologic observations suggest that the Campbellrand microbialites formed on a large, shallow marine platform covering the present Kaapvaal craton and its edge. The main microbialite buildups formed in shallow, subtidal to peritidal environments (Beukes, 1987; Sumner, 1997a). Our samples represent a range of depositional environments, including the distal slope of the platform. Hence, it is not surprising that the trace element and isotope signatures of the samples reflect an environment where open marine waters (those with the most juvenile isotope signatures) mixed with estuarine or lagoonal waters that were more influenced by relatively local continental hinterland. The implicit existence of poorly mixed water bodies is consistent with findings of earlier studies (e.g., Klein and Beukes, 1989; Beukes et al., 1990, Bau et al., 1997b, Sumner, 1997a). However, the present study found a stronger distinction between open marine and continent-dominated water chemistries, which clearly requires that relatively local erosion sources of crystalline rocks must have existed, an interpretation that conflicts with the view that the entire Kaapvaal craton had been covered with a thick carbonate blanket. However, Klein and Beukes (1989) noticed previously that "the location of a terrigenous source for the shales can only be speculated upon" and that "this source may have persisted throughout the deposition of the Campbellrand sequence." One probable catchment existed to the present northeast in the central zone of the Limpopo metamorphic belt, where Holzer et al. (1998) dated a high-grade metamorphic event to 2524 $\pm$ 5 Ma. Furthermore, it is likely that the continent to which the Kaapvaal craton belonged at 2.52 Ga was substantially larger, that is, the Vaalbara of Cheney (1996), but it is not possible to estimate the true extent of the Kaapvaal craton during deposition of the Campbellrand carbonates, because the western and northern margins of the craton were involved in 1.9 to 2.0 Ga orogenies (Duane and Kruger, 1991; Kamber et al., 1995).

The Nd-isotope composition of continental sources largely reflects the age of the eroded catchment. The most extreme Nd-isotope compositions today are found in rivers draining early Archaean shields, for example, Isua with $\varepsilon_{Nd}$ of $-44$ (Goldstein and Jacobsen, 1987). According to Jahn

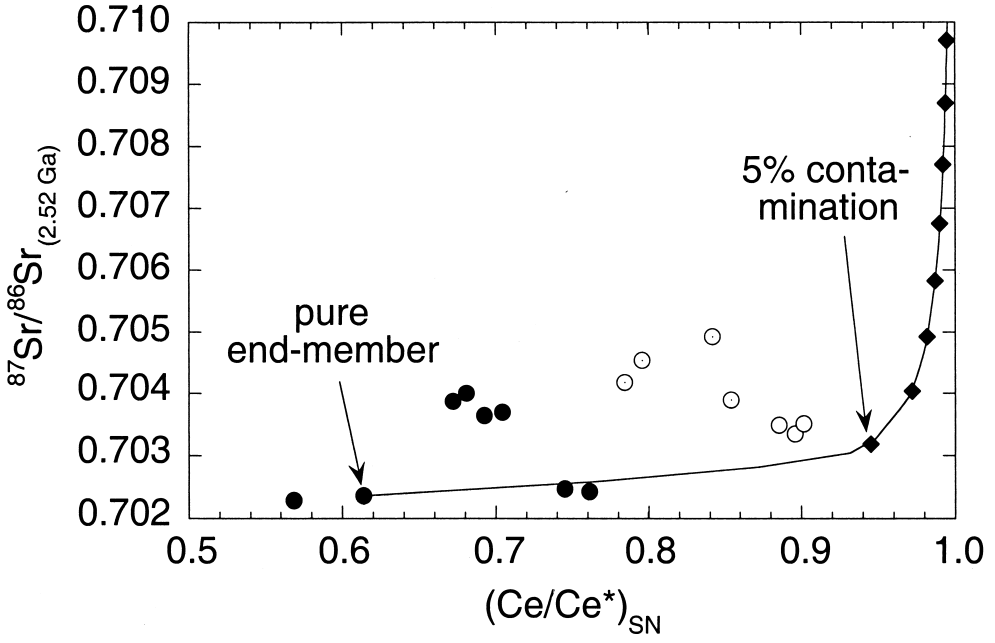


Fig. 7. Initial Sr-isotope ratio vs. La anomaly expressed as Ce/Ce* ($[Ce/0.5\ La + 0.5\ Pr]_{SN}$). Solid diamond symbols represent 5% mixing intervals between the contaminant (PAAS, McLennan, 1989) and a postulated pure endmember (sample 3b). Because no Sr concentration data are given for PAAS in McLennan (1989), an average was calculated from the Kaapvaal data of Jahn and Condie (1995), yielding median Sr and Nd concentrations of 30.5 ppm and 29.5 ppm, respectively. The good match with PAAS Nd concentration (33.9 ppm) validates the use of Kaapvaal shale Sr estimates. The initial Sr-isotope composition of PAAS was assumed to be 0.725. The main feature of the mixing line (solid line) is its strong hyperbolic curvature (note that the PAAS endmember plots far off scale). This reflects the large REE concentration contrast between the carbonate and PAAS, while Sr contents are similar in both endmembers. Therefore, even small degrees of contamination with shale lead to immediate and strong decrease in La anomaly (see also Fig. 2b). All Campbellrand carbonates with $^{87}Sr/^{86}Sr > 0.703$ plot clearly above the mixing line.

and Condie (1995), Nd-isotope systematics of pelites from the Kaapvaal craton indicate an absence of very old (i.e., > 3.6 Ga) erodible crust. Typical crustal residence times of material incorporated into Kaapvaal pelites before erosion ranged between 0.4 and 1.0 Ga, corresponding to Nd-isotope compositions at the time of deposition of between −8 and −1.5 $\varepsilon_{Nd}$. These values would indicate that the least radiogenic Campbellrand carbonates were strongly dominated by continental sources. The Sr-isotope composition of continental sources is more strongly dependent on the nature of eroded crust (i.e., the ratio between carbonate to silicate weathering in the catchment) than on crustal age. Continental Sr can evolve to very radiogenic compositions in < 1 Ga, and the most radiogenic Sr is presently found where older basement has recently been metamorphically reworked and is exposed in actively eroding mountain belts (e.g., Himalaya). Therefore, it is reasonable to suggest that at 2.5 Ga, rivers draining a catchment of ~0.6 Ga age, could have had $^{87}Sr/^{86}Sr$ ratios > 0.71 (e.g., Deb et al., 1991). However, if the continental runoff was dominated by eroded carbonate, the Sr-isotope composition could have been less radiogenic, that is, < 0.705 (Derry and Jacobsen, 1988). The Sr-isotope composition of the most radiogenic carbonates, which incidentally are the lagoon samples (Fig. 6a), again indicates a strong continental component, and denies a dominance of carbonate weathering in the catchment.

### 4.3. Implications for Hydrothermal vs. Continental Flux

The Nd-isotope composition of hydrothermal input can be approximated with that of MORB-source mantle, which at present has an average $\varepsilon_{Nd}$ of approximately +10. If a linear isotope evolution is assumed for the MORB-source mantle, hydrothermal input 2.52 Ga ago would have had an Nd-isotope composition of +4.5 $\varepsilon_{Nd}$. However, other models for the Nd-isotope evolution of the MORB-source mantle predict that the $\varepsilon_{Nd}$ of hydrothermal sources could have been as low as +2 (e.g., Nägler and Kramers, 1998). Sr that enters the ocean from hydrothermal systems along midocean ridges has a primitive isotope composition with a $^{87}Sr/^{86}Sr$ ratio of ~0.7027 (e.g., Allègre et al., 1983). The exact Sr-isotope evolution of the MORB-source mantle is unknown, but 2.5 Ga ago, the mantle $^{87}Sr/^{86}Sr$ ratio was likely to have been ~0.7015 (e.g., Zachariah, 1998). The mantle-like Sr-isotope composition of Archaean limestones was interpreted originally by Veizer and Compston (1976) to reflect a change in the "fractionation state of the contemporary crust." However, because the average composition of continental crust has not changed greatly since 3.7 Ga (e.g., Condie, 1993; Jahn and Condie, 1995), the phenomenon is better interpreted to reflect a change in the ratio between hydrothermal and continental flux to the oceans, that is, the flux ratio (Derry and Jacobsen, 1988). The value for hydrothermal flux at 2.52 Ga can be calculated from the isotope compositions of contemporary seawater ($^{87}Sr/^{86}Sr = 0.702386$,

this study), MORB-source mantle ($^{87}Sr/^{86}Sr = 0.70153$, caption to Fig. 6a), and eroded continental crust. For a sialic continental $^{87}Sr/^{86}Sr$ ratio of 0.70505 (which reflects a linear evolution from 0.6995 with a $^{87}Rb/^{86}Sr$ ratio of 0.1915 to the present day ratio of 0.7119), the flux ratio has a value of 3.1, strongly in favour of hydrothermal flux. That is six to 10 times higher than calculated Phanerozoic flux ratios (0.3–0.5). The most underconstrained parameters in the preceding calculations are the isotope compositions of dissolved Sr from the continents and that of the late Archaean oceans. Because Campbellrand carbonates provide only an upper limit to the Sr-isotope composition of coeval seawater, there is a possibility that the true Sr flux ratio was significantly greater than 3. For example, if the true $^{87}Sr/^{86}Sr$ ratio of 2.52 Ga seawater was 0.7018, the flux ratio would have been ~12.

Another approach is to calculate the flux ratio for a hypothetical anoxic modern Earth by relating the Nd and Sr flux ratios, provided that the Nd/Sr ratios in hydrothermal fluids and dissolved river loads can be estimated. The ratio between dissolved Sr and Nd in average world river water is well established at ~1500 (Goldstein and Jacobsen, 1987). The Sr/Nd ratio of endmember hot hydrothermal waters is less well constrained. Goldstein and Jacobsen (1987) estimated 11.4 ppm Sr and 700 ppt Nd concentrations from published data of hydrothermal waters of the East Pacific Rise. Klinkhammer et al. (1994) reported combined Sr and Nd data of vent fluids from a number of midocean ridges, and their average values of Sr and Nd contents are similar to earlier estimates (10.65 ppm Sr and 359 ppt Nd). The calculated Sr/Nd ratios are 16,300 (Goldstein and Jacobsen, 1987) and 29,700 (calculated from Klinkhammer et al., 1994). Because REE do not behave as conservative elements during mixing with ambient seawater, there is a possibility that extrapolation to Mg-free fluid compositions could underestimate the true REE content of vent fluid by ~50% (Bau and Dulski, 1999). Sr behaves conservatively and is not affected. To compensate for possible Nd underestimates (in studies such as Klinkhammer et al., 1994) we use an Sr/Nd ratio of 15,000 in the following calculation. The Nd flux ratio for a hypothetical anoxic modern ocean can simply be calculated by multiplying the modern Sr flux ratio (~0.5) with the ratio of the hydrothermal and riverine Sr/Nd ratios (i.e., 15,000/1500) to yield a value of 0.05. That value is very similar to the Goldstein and Jacobsen (1987) estimate of 0.042. In other words, only 4% to 5% of the dissolved Nd in the present ocean is derived from hydrothermal sources. Such a low contribution to the REE budget could under no circumstances explain the radiogenic Nd-isotope ratios and the positive Eu anomalies of the deeper Gamohaan carbonates.

Indeed, to obtain a seawater Nd-isotope composition of +2 $\varepsilon_{Nd}$ from likely inputs (+4.5 $\varepsilon_{Nd}$ hydrothermal and −5 $\varepsilon_{Nd}$ continental), an Nd flux ratio of 2.8 is required, which is a ~50-fold increase relative to present-day flux. That finding is in good agreement with the oceanic input calculations derived from combined REE and Nd-isotope data of Precambrian BIF by Derry and Jacobsen (1990).

Two robust conclusions can be drawn despite the uncertainties related to the assumptions used in our calculations. First, combined mass balance for Sr and Nd can be achieved only if the true $^{87}Sr/^{86}Sr$ of dissolved marine Sr at 2.52 Ga was $<$ 0.7024. Second, combined Nd- and Sr-isotope mass balance indicates a flux ratio that favours the hydrothermal flux by an order of magnitude. Such a large increase in hydrothermal flux is unlikely to have been caused solely by a change in the intensity of hydrothermal activity along spreading ridges even if the continental flux is reduced to 40%, reflecting the smaller continental volume at the time. Rather, it appears most likely that the change in flux ratio from 2.52 Ga to the present also involved a fundamental change in the erosion history of the continents.

### 4.4. Possible Causes for Reduced Archaean Continental Erosion Rates

Our interpretation that continental erosion flux in the Archaean was lower than at present (even after correction for reduced continental mass) adds to existing evidence that a fundamental change in exogenetic processes occurred during the early Proterozoic. Allègre and Rousseau (1984) interpreted the relatively sudden post-2.0 Ga deviation of Nd-isotope sediment model age from stratigraphic age to indicate an increase in continental erosion rates. The Kramers and Tolstikhin (1997) solution to both terrestrial Pb paradoxes requires increased erosion rates post-2.0 Ga, with strongest acceleration between 2.0 and 1.5 Ga. More recently, Collerson and Kamber (1999) found evidence for significantly decreased net continental growth rate post-2.0 Ga (inferred from MORB-source mantle Nb-Th-U systematics), which was interpreted to reflect an increase in erosion rates. There are a number of possible causes for reduced Archaean continental erosion, which can be grouped into two classes, tectonic and palaeoclimatic.

Galer and Mezger (1998) recently reviewed the interplay between sedimentary cycling, mean continental thickness, isostasy, and freeboard. The interplay is based on the concept of equilibration of continental thickness, which refers to the fact that as a particular continent becomes thicker (in the global isostatic framework), it rises relative to sea level and will be eroded accordingly. Conversely, when rifting thins a continent to a degree, it will subside and become a locus of sediment accumulation. As a result of such processes, the sedimentary cycle maintains continental thickness. On a tectonically active planet in the modern sense, orogenic cycles cause great differences in relative isostasy, which cause topographic variation and trigger the two complementary forces of the sedimentary cycle, erosion and deposition. Galer and Mezger (1998) concluded that the average longterm uplift and erosion experienced by Archaean greenstone terrains was a mere 5 km. The lack of evidence for large vertical movements of those shields (i.e., their shallow maximum burial depths) thus could be interpreted to reflect a tectonically placid Archaean planet. Other authors have argued that Archaean lower crust was more plastic than today, owing to changes in the thermal state of the planet (Choukroune et al., 1995). Therefore, the more plastic crust could not support the mass of a high orogenic edifice without lateral extrusion. In either case, the absence of preserved true Archaean eclogites and the comparatively thin greenstone stratigraphies are a good indication that the amount of vertical movement in Archaean continents was small.

Melezhik et al. (1997) stressed the importance for the exogenetic cycle of shallow, intracontinental rift basins, which constitute another dominant aspect of late Archaean/early Pro-

terozoic geology. The expansion of epicontinental seas not only provides an attractive explanation for accelerated microbialite evolution (Melezhik et al., 1997), related shifts in C-isotope balance, and potential Fe-Mn sinks (Eriksson, 1995), but such seas could also greatly reduce the continental flux to the open oceans. Even in modern estuaries, as much as 70% of Nd can be scavenged in the course of mixing saline with fresh waters (e.g., Goldstein and Jacobsen, 1987), and the impact of epicontinental seas, particularly on the flux ratio of Nd, is potentially large. More important than scavenging, perhaps, is that expansion of epicontinental seas could also reflect times of high sea levels, with the obvious direct reduction of erosion rates.

The timing inferred by some authors (Kramers and Tolstikhin, 1997; Collerson and Kamber, 1999) for a global increase in erosion rate (2.0–1.6 Ga) coincides with estimates for the establishment of a pandemic oxidising atmosphere. The influence of a change in atmospheric composition on global physical and chemical weathering rates is unknown, but is probably not the relevant issue. Weathering could cause development of deep regolith, but erosion of that regolith would require pronounced topographic relief (e.g., even today, very deep regoliths can persist for up to 75 Ma in tectonically stable areas; Vasconcelos, 1999).

## 5. SUMMARY

We have demonstrated previously the feasibility and validity of microbial carbonates as a proxy for shallow marine REE+Y chemistry (Webb and Kamber, 2000). In this paper we used the REE+Y geochemistry and isotope systematics of 2.52 Ga stromatolitic microbialites to test published, yet controversial claims for much stronger hydrothermal input in the Archaean oceans. A consistent picture results from three independent lines of evidence that all support the hypothesis of hydrothermally dominated, largely anoxic Archaean oceans: (1) the presence of a shale-normalised Eu anomaly coupled with the absence of a negative Ce anomaly, (2) initial Sr-isotope ratios that are much less radiogenic than those recorded in the Phanerozoic and only marginally more radiogenic than that of coeval mantle, and (3) superchondritic initial Nd-isotope ratios that cannot be attributed to artifacts caused by inappropriate Sm-decay correction because of good correlation with initial Sr-isotope ratios (that require almost no Rb-decay correction).

Trace element ratios and initial isotope compositions vary in the ancient samples. Mixing calculations indicate that much of the variability might reflect actual heterogeneity of the water chemistry rather than contamination of the marine signal by trapped detritus. If true, geochemistry of Campbellrand carbonates implies the existence of poorly mixed water masses with different chemistries. That interpretation is supported by the consistent correlation of water chemistry with depositional environment (i.e., deeper samples record relatively more hydrothermal signatures and lagoonal samples record relatively more estuarine signatures).

The main observation of a hydrothermally dominated oceanic flux ratio, however, is valid irrespective of the cause of chemical and isotopic variation. Similar claims for hydrothermal dominance in the Archaean oceanic trace element inventory have been made previously (e.g., Derry and Jacobsen, 1990; Bau et al., 1997b). However, in contrast to previous studies, we find it difficult to explain the Archaean flux ratio simply in terms of much-increased Archaean hydrothermal activity. Even if the continental flux is reduced in proportion to the contemporary continental volume (i.e., 40% relative to today), the required hydrothermal input is 10 times greater than that of today. Such an increase by far exceeds estimates for Archaean ridge length or oceanic crust production rates, which are both ultimately linked to Earth's cooling history. We therefore propose that the strong dominance of hydrothermal input into Archaean oceans also requires more limited continental erosion flux per continent volume than occurs today. Reasons for inhibited erosion remain speculative at this stage, but a secular change in the response of continents to isostatic forces (i.e., reduced topography) has the greatest potential to reduce erosion rates.

*Acknowledgments*—We thank Alan Greig for sharing ICP-MS skills and Nic Beukes for providing samples and for provoking interest in these issues. Michael Bau and Friedhelm von Blanckenburg contributed to many discussions. Thanks go to the journal reviewers, particularly Dawn Sumner, for very thoughtful reviews. This work was funded by Swiss National Science Foundation grant # 8220-050352 to B. S. K.

*Associate editor:* K. Kyser

## REFERENCES

Alibert C. and McCulloch M. T. (1993) Rare earth element and neodymium isotopic compositions of the banded iron formations and associated shales from Hamersley, western Australia. *Geochim. Cosmochim. Acta* **57,** 187–204.

Allègre C. J., Hart S. R., and Minster J. F. (1983) Chemical structure and evolution of the mantle and continents determined by inversion of Nd and Sr isotopic data, II. Numerical experiments and discussion. *Earth Planet. Sci. Lett.* **66,** 191–213.

Allègre C. J. and Rousseau D. (1984) The growth of the continents through time studied by Nd isotope analyses of shales. *Earth Planet. Sci. Lett.* **67,** 19–34.

Banner J. L., Hanson G. N., and Meyers W. J. (1988) Rare earth element and Nd isotopic variations in regionally extensive dolomites from the Burlington-Keokuk Formation (Mississippian): Implications for REE mobility during carbonate diagenesis. *J. Sedim. Petrol.* **58,** 415–432.

Bau M. (1999) Scavenging of dissolved yttrium and rare earths by precipitating iron oxyhydroxide: Experimental evidence for Ce oxidation, Y-Ho fractionation, and lanthanide tetrad effect. *Geochim. Cosmochim. Acta* **63,** 67–77.

Bau M. and Dulski P. (1996) Distribution of yttrium and rare-earth elements in the Penge and Kuruman iron-formations, Transvaal Supergroup, South Africa. *Precamb. Res.* **79,** 37–55.

Bau M. and Dulski P. (1999) Comparing yttrium and rare earths in hydrothermal fluids from the Mid-Atlantic Ridge: Implications for Y and REE behaviour during near-vent mixing and for the Y/Ho ratio of Proterozoic seawater. *Chem. Geol.* **155,** 77–90.

Bau M. and Möller P. (1993) Rare earth element systematics of the chemically precipitated component in Early Precambrian iron formations and the evolution of the terrestrial atmosphere-hydrosphere-lithosphere system. *Geochim. Cosmochim. Acta* **57,** 2239–2249.

Bau M., Möller P., and Dulski P. (1997a) Yttrium and lanthanides in eastern Mediterranean seawater and their fractionation during redox-cycling. *Marine Chem.* **56,** 123–131.

Bau M., Höhndorf A., Dulski P., and Beukes N. J. (1997b) Sources of rare-earth elements and iron in Paleoproterozoic iron-formations from the Transvaal Supergroup, South Africa: Evidence from neodymium isotopes. *J. Geol.* **105,** 121–129.

Beukes N. J. (1987) Facies relations, depositional environments and diagenesis in a major early Proterozoic stromatolitic carbonate plat-

form to basinal sequence, Campbellrand Subgroup, Transvaal Supergroup, southern Africa. *Sediment. Geol.* **54,** 1–46.
Beukes N. J., Klein C., Kaufman A. J., and Hayes J. M. (1990) Carbonate petrography, kerogen distribution, and carbon and oxygen isotope variations in an early Proterozoic transition from limestone to iron-formation deposition, Transvaal Supergroup, South Africa. *Econ. Geol.* **85,** 663–690.
Canfield D. E., Habicht K. S., and Thamdrup B. (2000) The. Archean sulfur cycle and the early history of atmospheric oxygen. *Science* **288,** 658–661.
Castanier S., Métayer-Levrel G., and Perthuisot J. P. (1999) Ca-carbonates precipitation and limestone genesis—the microbiogeologist point of view. *Sediment. Geol.* **126,** 9–23.
Cheney E. S. (1996) Sequence stratigraphy and plate tectonic significance of the Transvaal succession of southern Africa and its equivalent in Western Australia. *Precamb. Res.* **79,** 3–24.
Choukroune P., Bouhallier H., and Arndt N. T. (1995) Soft Archean lithosphere during periods of crustal growth or reworking. *J. Geol. Soc. London Spec. Publ.* **95,** 67–86.
Collerson K. D. and Kamber B. S. (1999) Evolution of the continents and the atmosphere inferred from Th-U-Nb systematics of the depleted mantle. *Science* **283,** 1519–1522.
Condie K. C. (1993) Chemical composition and evolution of the upper continental crust: Contrasting results from surface samples and shales. *Chem. Geol.* **104,** 1–37.
Danielson A., Möller P., and Dulski P. (1992) The europium anomalies in banded iron formations and the thermal history of the oceanic crust. *Chem. Geol.* **97,** 89–100.
Deb M., Hoefs J., and Baumann A. (1991) Isotopic composition of two Precambrian stratiform barite deposits from the Indian shield. *Geochim. Cosmochim. Acta* **55,** 303–308.
Derry L. A. and Jacobsen S. B. (1988) The Nd and Sr evolution of Proterozoic seawater. *Geophys. Res. Lett.* **15,** 397–400.
Derry L. A. and Jacobsen S. B. (1990) The chemical evolution of Precambrian seawater: Evidence from REEs in banded iron formations. *Geochim. Cosmochim. Acta* **54,** 2965–2977.
Duane M. J. and Kruger F. J. (1991) Geochronological evidence for tectonically driven brine migration during the early Proterozoic Kheis orogeny of southern Africa. *Geophys. Res. Lett.* **16,** 975–978.
Edmond J. M., Measures C., McDuff R. E., Chan L. H., Collier R., Grant Gordon L. I., and Corliss J. B. (1979) Ridge crest hydrothermal activity and the balances of the major and minor elements in the ocean: The Galapagos data. *Earth Planet. Sci. Lett.* **46,** 1–18.
Eriksson K. A. (1995) Crustal growth, surface processes, and atmospheric evolution of the early Earth. In *Early Precambrian Processes*, Vol. 95 (ed. M. P. Coward and A. C. Ries), pp. 11–26, Geol. Soc. Spec. Publ.
Farquhar J., Bao H. M., and Thiemens M. (2000) Atmospheric influence of Earth's earliest sulfur cycle. *Science* **289,** 756–758.
Fryer B. J., Fyfe W. S., and Kerrich R. (1979) Archaean volcanogenic oceans. *Chem. Geol.* **24,** 25–33.
Galer S. J. G. and Mezger K. (1998) Metamorphism, denudation and sea level in the Archaean and cooling of the Earth. *Precamb. Res.* **92,** 389–412.
German C. R., Holliday B. P., and Elderfield H. (1991) Redox cycling of rare earth elements in the suboxic zone of the Black Sea. *Geochim. Cosmochim. Acta* **55,** 3553–3558.
Goldstein S. J. and Jacobsen S. B. (1987) The Nd and Sr isotopic systematics of river-water dissolved material: implications for the sources of Nd and Sr in seawater. *Chem. Geol.* **66,** 245–272.
Hälbich I. W., Lamprecht D., Altermann W., and Horstmann U. E. (1992) A carbonate-banded iron formation transition in the Early Proterozoic of South Africa. *J. African Earth. Sci.* **15,** 217–236.
Holzer L., Frei R., Barton J. M., and Kramers J. D. (1998) Unraveling the record of successive high grade events in the Central Zone of the Limpopo Belt using Pb single phase dating of metamorphic minerals. *Precamb. Res.* **87,** 87–115.
Jacobsen S. B. and Pimentel-Klose M. R. (1988) Nd isotopic variations in Precambrian banded iron formations. *Geophys. Res. Lett.* **15,** 393–396.
Jahn B. M. and Condie K. C. (1995) Evolution of the Kaapvaal Craton as viewed from geochemical and Sm-Nd isotopic analyses of intracratonic pelites. *Geochim. Cosmochim. Acta* **59,** 2239–2258.
Kamber B. S., Kramers J. D., Napier R., Cliff R. A., and Rollinson H. R. (1995) The Triangle Shearzone, Zimbabwe, revisited: New data document an important event at 2.0 Ga in the Limpopo Belt. *Precamb. Res.* **70,** 191–213.
Klein C. and Beukes N. J. (1989) Geochemistry and sedimentology of a facies transition from limestone to iron formation deposition in the early Proterozoic Transvaal Supergroup, South Africa. *Econ. Geol.* **84,** 1731–1774.
Klinkhammer G. P., Elderfield H., Edmond J. M., and Mitra A. (1994) Geochemical implications of rare earth element patterns in hydrothermal fluids from mid-ocean ridges. *Geochim. Cosmochim. Acta* **58,** 5105–5113.
Kramers J. D. and Tolstikhin I. N. (1997) Two terrestrial lead isotope paradoxes, forward transport modelling, core formation and the history of the continental crust. *Chem. Geol.* **139,** 75–110.
McLennan S. M. (1989) Rare earth elements in sedimentary rocks: Influence of provenance and sedimentary processes. In *Geochemistry and Mineralogy of Rare Earth Elements*, Vol. 21 (ed. B. R. Lipin and G. A. McKay), pp. 169–200, Mineral Society of America.
Melezhik V. A., Fallick A. E., Makarikhin V. V., and Lyubtsov V. V. (1997) Links between Palaeoproterozoic palaeogeography and rise and decline of stromatolites: Fennoscandian Shield. *Precamb. Res.* **82,** 311–348.
Michard A. and Albarède F. (1986) The REE content of some hydrothermal fluids. *Chem. Geol.* **55,** 51–60.
Miller R. G. and O'Nions R. K. (1985) Source of Precambrian chemical and clastic sediments. *Nature* **314,** 325–329.
Mirota M. D. and Veizer J. (1994) Geochemistry of Precambrian carbonates: VI. Aphebian Albanel Formations, Quebec, Canada. *Geochim. Cosmochim. Acta* **58,** 1735–1745.
Mitra A., Elderfield H., and Greaves M. J. (1994) Rare earth elements in submarine hydrothermal fluids and plumes from the Mid-Atlantic Ridge. *Marine Chem.* **46,** 217–235.
Moorbath S., Taylor P. N., Orpen J. L., Treloar P., and Wilson J. F. (1987) First direct radiometric dating of Archaean stromatolitic limestone. *Nature* **326,** 865–867.
Nägler T. F. and Kramers J. D. (1998) Nd isotopic evolution of the upper mantle during the Precambrian: Models, data and the uncertainty of both. *Precamb. Res.* **91,** 233–252.
Nozaki Y., Zhang J., and Amakawa H. (1997) The fractionation between Y and Ho in the marine environment. *Earth Planet. Sci. Lett.* **148,** 329–340.
Parekh, P. P., Möller, P., Dulski, P., and Bausch, W. M. (1977) Distribution of trace elements between carbonate and non-carbonate phases of limestone. *Earth Planet. Sci. Lett.* **34,** 39–50.
Riding R. (1991) Classification of microbial carbonates. In *Calcareous Algae and Stromatolites* (ed. R. Riding), pp. 21–51, Springer.
Schieber J. (1988) Redistribution of rare-earth elements during diagenesis of carbonate rocks from the mid-Proterozoic Newland Formation, Montana, U.S.A. *Chem. Geol.* **69,** 111–126.
Scherer M. and Seitz H. (1980) Rare-earth element distribution in Holocene and Pleistocene corals and their redistribution during diagenesis. *Chem. Geol.* **28,** 279–289.
Shaw H. F. and Wasserburg G. J. (1985) Sm-Nd in marine carbonates and phosphates: Implications for Nd isotopes in seawater and crustal ages. *Geochim. Cosmochim. Acta* **49,** 503–518.
Shimizu H., Umemoto N., Masuda A., and Appel P. W. U. (1990) Sources of iron-formations in the Archean Isua and Malene supracrustals, West Greenland: Evidence from La-Ce and Sm-Nd data and REE abundances. *Geochim. Cosmochim. Acta* **54,** 1147–1154.
Sumner D. Y. (1997a) Carbonate precipitation and oxygen stratification in late Archean seawater as deduced from facies and stratigraphy of the Gamohaan and Frisco Formations, Transvaal Supergroup, South Africa. *Am. J. Sci.* **297,** 455–487.
Sumner D. Y. (1997b) Late Archean calcite-microbe interactions: Two morphologically distinct microbial communities that affected calcite nucleation differently. *Palaios.* **12,** 302–318.
Sumner D. Y. and Bowring S. A. (1996) U-Pb geochronologic constraints on deposition of the Campbellrand Subgroup, Transvaal Supergroup, South Africa. *Precamb. Res.* **79,** 25–35.
Terakado Y. and Masuda A. (1988) The coprecipitation of rare-earth elements with calcite and aragonite. *Chem. Geol.* **69,** 103–110.

Vasconcelos P. M. (1999) K-Ar and $^{40}Ar/^{39}Ar$ geochronology of weathering processes. *Annu. Rev. Earth Planet. Sci.* **27,** 183–229.

Veizer J. and Compston W. (1976) $^{87}Sr/^{86}Sr$ in Precambrian carbonates as an index of crustal evolution. *Geochim. Cosmochim. Acta* **40,** 905–914.

Veizer J., Compston W., Hoefs J., and Nelsen H. (1982) Mantle buffering of the early oceans. *Naturwissenschaften* **69,** 173–180.

Viers J., Dupré B., Polvé M., Schott J., Dandurand J. L., and Braun J. J. (1997) Chemical weathering in the drainage basin of a tropical watershed (Nsimi-Zoetele site, Cameroon): Comparison between organic-poor and organic-rich waters. *Chem. Geol.* **140,** 181–206.

Webb G. E. and Kamber B. S. (2000). Rare earth elements in Holocene reefal microbialites: A new shallow seawater proxy. *Geochim. Cosmochim. Acta* **64,** 1557–1565.

Wilks M. E. and Nisbet E. G. (1988) Stratigraphy of the Steep Rock Group, northwest Ontario: A major Archaean unconformity and Archaean stromatolites. *Can. J. Earth Sci.* **25,** 370–391.

Zachariah J. K. (1998) A 3.1 billion year old marble and the $^{87}Sr/^{86}Sr$ of late-Archean seawater. *Terra Nova* **10,** 312–316.

Zhong S. and Mucci A. (1995) Partitioning of rare earth elements (REEs) between calcite and seawater solutions at 25°C and 1 atm, and high dissolved REE concentrations. *Geochim. Cosmochim. Acta* **59,** 443–453.